



## Mutation in *cyl* operon alters hemolytic phenotypes of *Streptococcus agalactiae*

Chin Cheng Chou, Men Chieng Lin, Feng Jie Su, Meei Mei Chen\*

Department of Veterinary Medicine, National Taiwan University, Taipei, Taiwan



### ABSTRACT

*Streptococcus agalactiae* infects numerous fish species, causing considerable economic losses during fish cultivation. This study compared the phenotypic differences among *S. agalactiae* hemolytic variant isolates and investigated the genetic composition of their hemolysin genes. Hemolysin is encoded by the *cyl* operon and mainly regulated by *covS/R*, which also regulates encapsulation. In total, 45 *S. agalactiae* clinical isolates were collected from cultured fishes in Taiwan. Three different hemolytic phenotypes— $\alpha$ ,  $\beta$ , and  $\gamma$ —were identified. Of the 45 isolates, 39 were  $\beta$  hemolytic, 3 were  $\alpha$  hemolytic, and 3 were  $\gamma$  hemolytic. The  $\gamma$ -hemolytic isolates demonstrated significantly thicker encapsulation and slower growth rates than did the  $\alpha$ - and  $\beta$ -hemolytic isolates. However, no isolate had mutations in the regulatory gene *covS/R*. A 1252-bp insertion sequence (IS) in the *cyl* operon of  $\alpha$ -hemolytic isolates, located at *cylF* region, was found. This IS interrupted *cylF* through insertion at 23 bp downstream of starting codon, causing incomplete mRNA transcription. The  $\beta$ -hemolytic isolates showed no mutation in the *cyl* operon. By contrast, the  $\gamma$ -hemolytic isolates had lost the entire *cyl* operon; it had been replaced by a 14-kb genomic island containing genes for DNA recombinase and septum formation proteins. In summary, the differences in hemolysin genes between  $\alpha$ - and  $\beta$ -hemolytic isolates were due to the IS in the *cylF* region, whereas in the  $\gamma$ -hemolytic isolates, the entire *cyl* operon was deleted and replaced. These findings explain different hemolysin expressions of the clinical *S. agalactiae* isolates taken from fish ponds in Taiwan.

**Importance:** *Streptococcus agalactiae* infects both warm- and cold-blooded animals and causes major aquatic cultivation loss. Pathogenic isolates from the outbreak of fish ponds were examined their *cyl* operon gene.  $\alpha$ -Hemolytic isolate with mutant *cyl* operon was observed for the first time in aquaculture animals and was compared to intact or entire *cyl* operon deletion of  $\beta$ - and  $\gamma$ -hemolytic isolates. Hemolysin expression levels of *Streptococcus agalactiae* are explained.

### 1. Introduction

*Streptococcus agalactiae*, the only member of Lancefield group B (Group B streptococcus, GBS), has many phenotypes and genotypes. GBS causes neonatal sepsis, meningitis, and pneumonia in humans (Verani et al. 2010; Edwards and Nizet, 2011; Rodriguez-Granger et al. 2012). It can infect both warm- and cold-blooded animals (Garcia et al. 2008). GBS infects fresh, brackish, and saltwater fish, including Nile tilapia (*Oreochromis niloticus*), rainbow trout (*Oncorhynchus mykiss*), grey mullet (*Mugil cephalus*), and hybrid striped seabass (*Morone saxatilis*), and thus cause major cultivation loss (Evans et al. 2004; Garcia et al. 2008). Affected fish may show clinical signs of exophthalmia, corneal opacity, erratic swimming, darkening ascites, hemorrhage in the fin base or body, meningitis, and bacterial septicemia (Yanong and Francis-Floyd, 2010). Acute infection can cause mortality higher than 50% over a period of 3–7 days (Yanong and Francis-Floyd, 2010).

Exopolysaccharide capsule and  $\beta$ -hemolysin/cytolysin ( $\beta$ -h/c) are the two important virulence factors characterized in GBS. The exopolysaccharide capsule, which has low immunogenicity, prevents attacks from the host immune system. Moreover, sialic acid incorporated in the capsule increases immune resistance by inhibiting complement

activation and reducing opsonophagocytic clearance (Koskiniemi et al. 1998).  $\beta$ -hemolysin, a strong exotoxin, causes direct lysis of various eukaryotic cells, such as fibroblasts and lung epithelial cells (Nizet et al. 1996; Tapsall and Phillips 1991). In GBS,  $\beta$ -hemolysin production is encoded by a 12-kb gene cluster called the *cyl* operon, containing 12 genes: *cylX*, *cylD*, *cylG*, *acpC*, *cylZ*, *cylA*, *cylB*, *cylE*, *cylF*, *cylI*, *cylJ*, and *cylK*. These genes encoded enzymes involve in  $\beta$ -hemolysin biosynthesis (Whidbey et al. 2013). Gene mutation in the *cyl* operon results in the emergence of nonhemolytic GBS strains (Spellerberg et al. 1999, 2000; Sigge et al. 2008). Genetic analysis of the *cyl* operon is essential when investigating the phenotypic transformation of GBS hemolysin.

Transcriptional regulation of the *cyl* operon is mainly controlled by the two-component regulatory system (TCS) through the regulatory gene *covS/R*. This system can inhibit the expression of the *cyl* operon according to environmental stimulation. Complete deletion of *covS/R* causes GBS to become highly hemolytic with thinner encapsulation; moreover, the gene mutation of *covS/R* can simultaneously affect the hemolysis and encapsulation of GBS (Lamy et al. 2004; Jiang et al. 2005). Thus, a genetic analysis of *covS/R* is necessary to clarify the contributions of virulence factors, such as hemolysin, to the GBS variants. This study collected GBS strains from outbreaks at different fish

\* Corresponding author at: Department of Veterinary Medicine, National Taiwan University, No. 1, Section 4, Roosevelt Road, Taipei 106, Taiwan.  
E-mail address: [cmm@ntu.edu.tw](mailto:cmm@ntu.edu.tw) (M.M. Chen).

**Table 1**  
Characteristics of the species, origin, isolate number, type of hemolysin and capsule serotype of *S. agalactiae* isolates.

Family	Species	Origin <sup>a</sup>	Isolate number	Type of hemolysin	Capsule serotype
Cichlidae	<i>Oreochromis mossambicus</i>	N	1	β	Ia
			1	γ	Ib
		M	19	β	Ia
		1	γ	Ib	
		S	6	β	Ia
		1	γ	Ib	
	<i>Melanochromis auratus</i>	S	1	α	Ia
	<i>Pseudotropheus zebra</i>	S	1	α	Ia
Terapontidae	<i>Scortum barcoo</i>	M	2	β	Ia
	<i>Bidyanus bidyanus</i>	M	3	β	Ia
Percichthyidae	<i>Lateolabrax japonicus</i>	M	1	β	Ia
	<i>Maccullochella peelii</i>	S	1	β	Ia
Moronidae	<i>Morone saxatilis</i>	M	1	β	Ia
Latidae	<i>Lates calcarifer</i>	S	1	α	Ia
			1	β	Ia
Mygilidae	<i>Mugil cephalus</i>	M	1	β	Ia
Carangidae	<i>Trachinotus blochii</i>	S	1	β	Ia
Sparidae	<i>Acanthopagrus latus</i>	M	1	β	Ia
Polynemidae	<i>Eleutheronema rhadinum</i>	S	1	β	Ia

<sup>a</sup> : N: North part of Taiwan (Taipei), M: Middle part of Taiwan (Chiayi), S: South part of Taiwan (Tainan, Kaohsiung, Pingtung).

farms and identified three specific phenotypic variants of GBS. Genetic and functional analysis may provide further insight into the appearance of these variants.

## 2. Materials and methods

### 2.1. Source of bacteria and hemolytic isolates

In total, 45 GBS isolates were collected from different outbreaks at Taiwan fish farms. The GBS were then isolated on blood agar and incubated at 28 °C; this was followed by Gram staining and bacteria 16S rRNA identification (Table 1). Three of each hemolysin isolate type were selected: KS103F-0135 (KS), TN103-SF681 (TN681), and TN103-SF722 (TN722) for α-hemolytic isolates; CY0726-7 (0726-7), CY0728-4 (0728-4), and CY0728-5 (0728-5) for β-hemolytic isolates; and CY0815-3-c (0815-3), T2-G (T2G), and TN100F570 (TN) for γ-hemolytic isolates.

### 2.2. Bacterial identification

Bacteria were cultured at 28 °C in brain heart infusion (BHI) medium overnight and further pelleted at 5000 ×g for 10 min. Each pellet was suspended in 160 μL of distilled water; 40 μL of lysozyme (100 mg/mL) was then added and the pellet was digested at 37 °C for 30 min. In case of isolates showing thick encapsulation, the pellet was suspended in 176 μL of distilled water and mixed with 20 μL of lysozyme and 4 μL of mutanolysin (Sigma, USA), and the combined mass was incubated at 37 °C for 1 h. Bacterial DNA was extracted with a Gene plus mini-Blood & Tissue genomic DNA extraction kit (Viogene, Taiwan), used according to manufacturer instructions. Polymerase chain reaction (PCR) was used to amplify the 16S rRNA gene using specific primer pairs (Domeenech et al. 1996) and PCR reagents (Biotools, Spain). The following PCR protocol was used: 30 cycles of 94 °C for 1 min, followed by 58 °C for 1 min and then 72 °C for 90 s; finally,

72 °C for 10 min to complete the reaction. The PCR products (5 μL) were analyzed through gel electrophoresis and sequencing analysis.

### 2.3. Capsule analysis

To observe the capsule thickness, a 5-μL drop of 50% India ink (Becton Dickinson Co, USA) was added to a slide with Gram-stained bacteria according to manufacturer's instruction and mounted a coverslip on the top of the slide. The slide was observed with light microscope under an oil immersion lens at 1000×. The capsular serotype was identified through PCR (Poyart et al. 2007; Imperi et al. 2010). Ia- and Ib-specific gene regions were amplified from bacteria genomic DNA. The following PCR protocol was used: 94 °C for 3 min, followed by 30 cycles of 94 °C for 45 s, 55 °C for 30 s, and 72 °C for 90 s; finally, 72 °C for 10 min to complete the reaction. The PCR products (5 μL) were analyzed through gel electrophoresis.

### 2.4. Measurement of growth dynamics

Bacteria were cultured in BHI broth overnight. The cultured medium was adjusted to an optical density of 0.5 at 600 nm (OD<sub>600</sub>); next, 100 μL of this medium was inoculated into 50 mL of BHI broth and incubated at 28 °C with 250 rpm shaking. To determine the bacterial growth rate, OD<sub>600</sub> of 1 mL of the growing culture was read every 6 h until 72 h of inoculation were completed. The measurement was performed in triplicate and bacteria growth curves were drawn.

### 2.5. Genetic analysis—PCR

PCR was used to amplify the *cyl* gene regions by Cyl+, CylXG, CylDG, CylGA, CylBE, and CylE primers (Spellerberg et al. 1999). The entire *cyl* operon was amplified by using the primer rD2 (Table 2). The two-component regulatory gene region *covS/R* was amplified using the primer CovS/R (Lamy et al. 2004). The amplified *cyl* regions are shown in Fig. 3. Genomic DNA was used as a template for PCR. The following PCR conditions were used for amplifying *cyl* operon genes and *covS/R*: 94 °C for 3 min, followed by 35 cycles of 94 °C for 1 min, 50 °C–58 °C for 1 min, and 72 °C for 3 min; finally, 72 °C for 10 min to complete the reaction. For amplifying the entire *cyl* operon, GoTaqR Long PCR Master Mix (Promega, USA) was used, along with the following

**Table 2**  
Designed primer pairs used in this study.

Primer	Sequence 5' → 3'	Ta (°C)
CylFI	F: AAATGCTGCAAATTGAAGGAA	58 °C, 62.5 °C (nested-PCR)
	R: CTCCCACAATATCATGATAAGCC	
CylII	F: GTTCCTGAGCAATACAAA	56 °C, 61.2 °C (nested-PCR)
	R: ATGAAAATCCAACTGAC	
CylJK	F: GGAAGAAGGCAGTTAGTT	56 °C, 61.2 °C (nested-PCR)
	R: TGTCAATGGCAAATGTTA	
CylE1	F: TTGCGTAGTCACCTCCCT	50 °C
	R: GCCTCCTCCGATGATGCT	
CylF	F: AGCCTTAGACCTTGTGAT	50 °C
	R: TGTTCTGAAGCGAGTTT	
CylES	F: AGCAACTACCAAGCGTC	50 °C
	R: TGCCTTTTCTGACGAT	
CylIS	F: TTTCCACTGACTTATCA	50 °C
	R: AAGGCTTCTCACATTC	
CylIr	F: AGCATAAACAGCATCTC	50 °C
	R: AACCTTCTATCCCAATC	
CylJKr	F: GCTTTGGTACTTCAATTT	50 °C
	R: TGGGAGCATAGGTTAGA	
rD2	F: CTTGTGGGCTCTTGGTCA	50 °C
	R: GCGAGTAAAATCCCGTC	
rSD1	F: CAGGGTTCGGGTCGTAA	50 °C
	R: CCGCCAAGTGAGTGAGC	
rSD2	F: CCTAAAGGTATGCCAGCTA	50 °C
	R: CCTCATAAACGGATTGC	

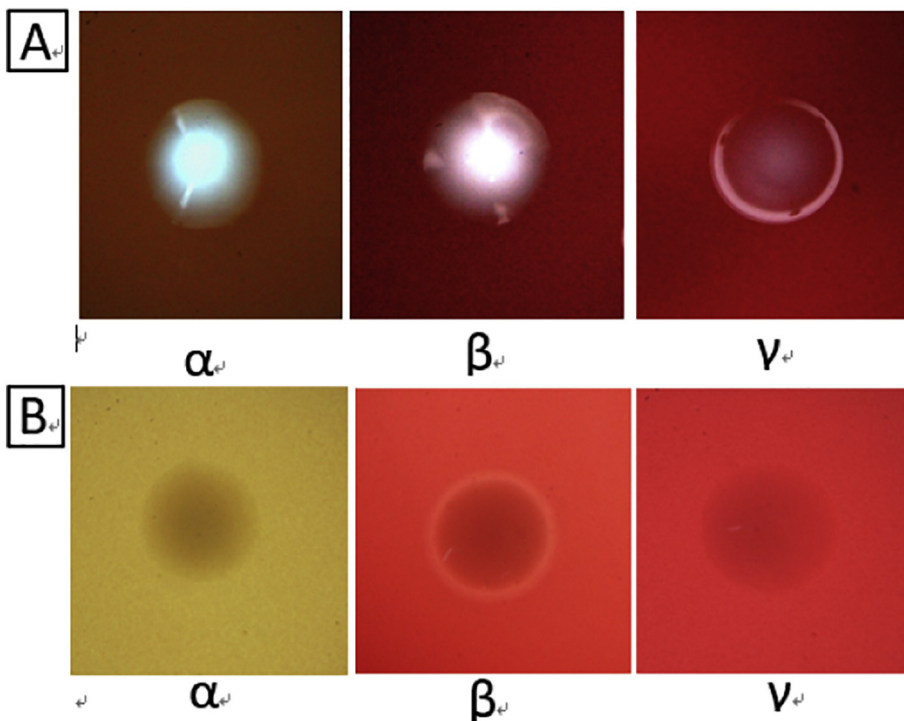


**Fig. 1.** A) Colonies shown on the surface of blood agar plates after 48 h incubation.  $\alpha$  and  $\beta$  hemolytic isolates showed white color colony, while  $\gamma$  hemolytic isolates showed relative translucent and sticky colony. B) Hemolytic activity of colonies on blood agar plates after 48 h incubation. The surrounding medium of the  $\alpha$  hemolytic isolate showed a greenish color alteration.  $\beta$  hemolytic isolate had a clear and colorless hemolytic zone surrounding the colony.  $\gamma$  hemolytic isolate had neither color alteration of the medium nor hemolytic zones.

protocol: 94 °C for 2 min, followed by 35 cycles of 94 °C for 30 s, 50 °C for 30 s, and 72 °C for 7 min; finally, 72 °C for 10 min to complete the reaction. All PCR products were analyzed through gel electrophoresis and sequencing.

## 2.6. Bacteria total RNA isolation and cDNA synthesis

Bacteria were cultured in BHI broth at 28 °C for 6–7 h. One milliliter of  $OD_{600} = 0.4$  culture was pelleted at 5000  $\times g$  for 10 min. Total RNA was extracted from the *S. agalactiae* pellet with TRIzol reagent (Invitrogen, USA) according to manufacturer instructions. The extracted RNA was treated with DNase I (Sigma, USA) to remove any genomic DNA that might interfere with PCR. Total RNA was quantified by determining absorbance at 260 nm, and 0.5  $\mu g$  of the bacterial RNA was used for cDNA synthesis. A PrimeScript 1st strand cDNA Synthesis Kit (TAKARA Bio, Japan) was used for reverse transcription, according to manufacturer instructions.

## 2.7. Genetic analysis—nested PCR

As described by Brown (2006), nested PCR was used to amplify *cyl* gene regions from the entire *cyl* operon synthesized by cDNA from ECOSTM 101 competent cells (Yeastern Bio, Taiwan). The primers used for *cyl* operon gene regions of  $\alpha$ - and  $\beta$ -hemolytic strains were CylXG, CylDG, CylGA, CylBE, CylE, CylFI (Spellerberg et al. 1999), CylI, CylJK, and rD2 (Table 2). The amplified gene regions are shown in Fig. 3. For  $\gamma$ -hemolytic isolates, specific primers for a 14-kb genomic island (GI), including DF (rD2-F and rSD2-R), DR (rSD2-F and rD2-R), and SD1 (rSD1-F and rSD1-R) were used (Table 2). The amplified gene regions are shown in Fig. 7A. The synthesis products for the entire *cyl* gene were used as templates, and nested PCR was performed using following conditions: 94 °C for 3 min, followed by 35 cycles of 94 °C for 1 min, 50 °C–62.5 °C for 1 min and 72 °C for 3 min; finally, 72 °C for 10 min to complete the reaction. The PCR products were analyzed through gel electrophoresis and sequencing.

## 2.8. Genetic analysis—reverse transcription PCR

Total RNA were reversed to cDNA according to PCR amplification with the following primer sets: CylE1, CylF, CylES, CylIS, CylIr, and CylJKr (Table 2). PCR was performed using the following conditions: 94 °C for 3 min, followed by 35 cycles of 94 °C for 1 min, 50 °C for 1 min, and 72 °C for 3 min; finally, 72 °C for 10 min to complete the reaction. The PCR products were analyzed through gel electrophoresis and sequencing.

## 2.9. Sequencing and primer design

All products were sequenced by Sanger sequencing (Mission Biotech in Taiwan), and analyzed using Basic Local Alignment Search Tool (BLAST) of National Center for Biotechnology Information (NCBI), USA. Primers were designed by Primer Premier 5.0 and synthesized by Mission Biotech.

## 2.10. Statistical analysis

Groups were compared by using the F test and Student's *t*-test. *P* values of < 0.05 and < 0.001 were considered significant and extremely significant, respectively. The standard deviation and standard error of the mean were calculated by using STDEV-P and STDEV-P/SQRT, respectively. Statistical calculations were performed in MS Excel 2010.

## 3. Results

### 3.1. Hemolytic activity and capsule analysis

Cultures on blood agar plate displayed GBS colonies with three different phenotypes- including  $\alpha$ ,  $\beta$  and  $\gamma$  hemolytic. Each hemolytic phenotype had three isolates. The surface of the colony and hemolytic activity were shown in Fig. 1. Evaluation of encapsulation by Indian ink showed higher encapsulation for  $\gamma$  hemolytic isolate comparing with  $\alpha$  and  $\beta$  hemolytic isolates (Fig. 2).

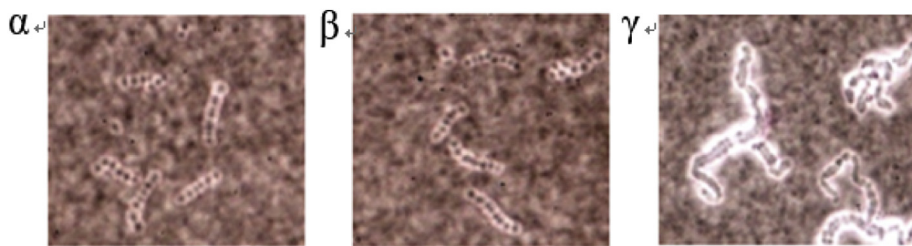


Fig. 2. Indian ink staining of the three hemolytic isolates observed with light microscope under an oil immersion lens at 1000×. α hemolytic and β hemolytic isolates both showed an indistinguishable blank space surrounding the bacteria after staining with Indian ink while γ hemolytic isolate showed thicker blank space surrounding the bacteria.

3.2. Isolation and growth curves of different hemolytic isolates

Based on the sequence alignment of the 16S rRNA gene, all the isolates were gram-positive cocci demonstrating 99% identity with *S. agalactiae*. The α- and β-hemolytic bacteria on the surface of blood agar plates after 48 h culture had white colony but the γ-hemolytic isolates appeared translucent and sticky. Because of their hemolytic activity, α-hemolytic isolates formed a greenish zone around their colonies, whereas β-hemolytic isolates formed a clear, colorless hemolytic zone. However, γ-hemolytic isolates neither altered the medium color nor formed hemolytic zones. The γ-hemolytic isolates showed relative thicker encapsulation than did the α- and β-hemolytic isolates. Both α- and β-hemolytic isolates belonged to capsular serotype Ia, whereas γ-hemolytic isolates belonged to capsular serotype Ib (Table 1). Fig. 4 illustrates that the growth of the γ-hemolytic isolates was slower than that of α- and β-hemolytic isolates: to reach the stationary phase, the α- and β-hemolytic isolates required only 18 h, but the γ-hemolytic isolates required 48 h. The growth curves of the α- and β-hemolytic isolates did not differ. By contrast, after 6 h of culturing, the growth of the γ-hemolytic isolates showed significant differences from the growth of the α- and β-hemolytic isolates.

3.3. Identification of *cyl* genes from three hemolytic isolates

To determine whether genetic mutations could explain the observed phenotypic differences, the genes implicated in β-h/c production or regulation were sequenced. The amplification and sequencing of the primers Cyl+, CylXG, CylDG, CylGA, CylBE, CylFI, CylI, and CylJK showed no difference between the α- and β-hemolytic isolates; however, a variation in the amplicon of primer CylE was noted: the amplicon was 1865-bp long for the β-hemolytic isolates but about 3000-bp long for the α-hemolytic isolates (Fig. 5). Nevertheless, none of these amplicons were observed in the γ-hemolytic isolates. The published sequence of the serotype Ia genome strain CNCTC 10/84 (CP006910) was identical to that of the α- and β-hemolytic isolates.

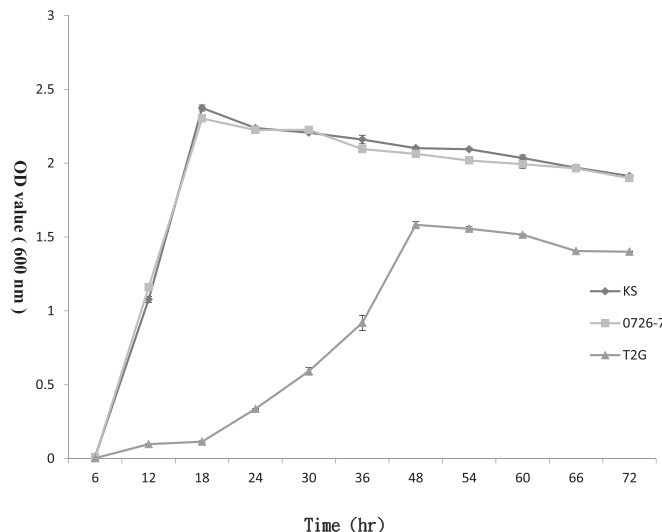


Fig. 4. Growth curve of group B streptococcal α (KS), β (0726–7) and γ (T2G) hemolytic variants in BHI broth at 28 °C. The experiments carried on the growth curves were through three colonies each times for different hemolytic isolates and repeated three times. Data were given as mean ± SD. Detection absorbance at 600 nm.

3.4. The insertion sequence (IS) in a hemolytic isolate *cyl* gene

Sequencing of primer CylE amplicon for the α-hemolytic isolates revealed a 1252-bp DNA fragment at 23 bp downstream of the ATG start codon of the *cylF* region. The insertion sequence (IS) started from nucleotide 63 to 1314 and was identified with IS3 family (Fig. 6A). The IS3 family normally contains two open reading frames, *orfA* and *orfB*. The IS in our study contained two consecutive open reading frames of 275 and 432 bp, which ran from nucleotide 487 to 761 and from nucleotide 837 to 1268, respectively, and were designated as *orfA'* and *orfB'*, respectively. In addition, the IS was flanked by 36-bp non-perfect

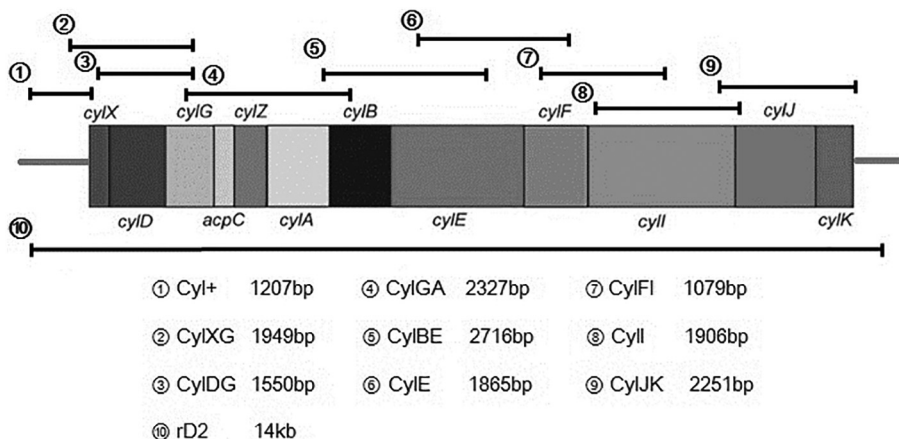
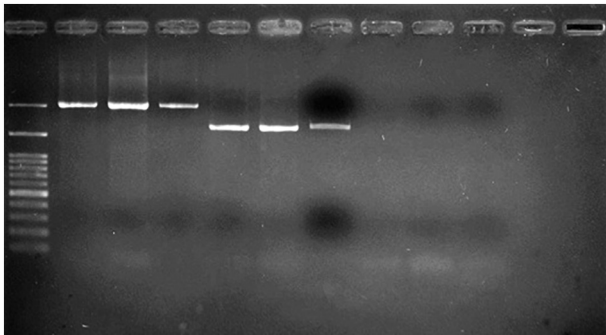
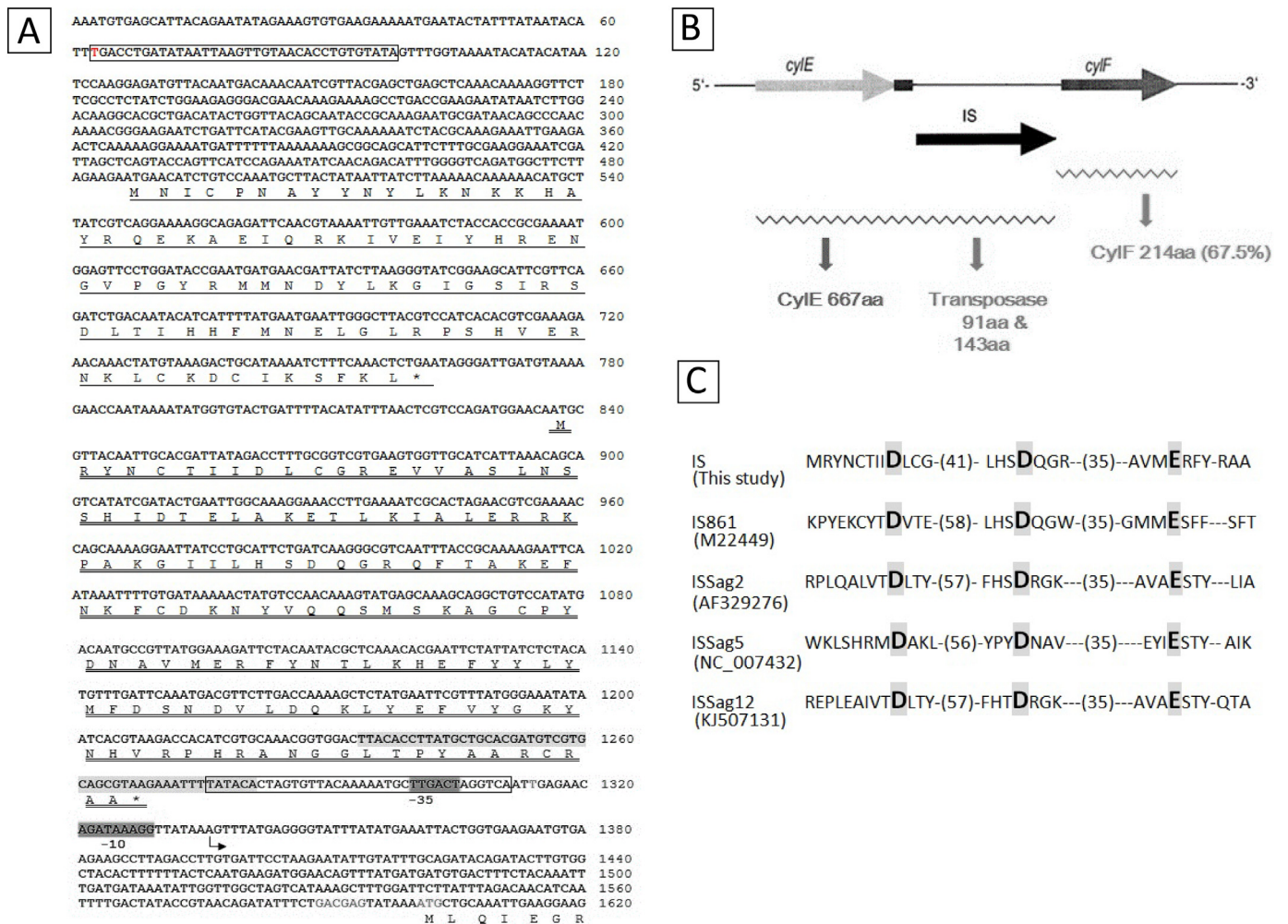


Fig. 3. Amplified gene regions for detecting *cyl* operon genes.



**Fig. 5.** Identification of *cyl* genes by PCR with primer *CylE*. DNA from three hemolytic isolates were used as templates. Lane 1–3 were  $\alpha$  hemolytic isolates KS, TN681 and TN722. Lane 4–6 were  $\beta$  hemolytic isolates 0726-7, 0728-4 and 0728-5. Lane 7–9 were  $\gamma$  hemolytic isolates 0815-3, T2G and TN. N as negative control. Positive 1865 bp amplicons were seen in  $\beta$  hemolytic isolates (shown by arrow), and about 3000 bp amplicons were seen in  $\alpha$  hemolytic isolates (shown by crude arrow). No amplicon was seen in  $\gamma$  hemolytic isolates.



**Fig. 6.** The insertion sequence (IS) in  $\alpha$  hemolytic isolate gene. A) DNA sequences of IS, starting from nucleotides 63 to 1314. The inverted repeats were indicated as open boxes, and the two open reading frames *orfA'* and *orfB'* were underlined and double-underlined, respectively. The transcriptional terminator was shown as shaded boxes. The putative  $-35$  and  $-10$  promoter regions were from nucleotides 1300 to 1305 and 1321 to 1329, respectively. Transcription start site was marked as arrow. Ribosome-binding site and start codon of downstream *CylF* protein were also shown. B) Graphic representation of the putative *CylE* and *CylF* and the insertion site of IS. The putative transcriptional mRNA was shown as meander line, and putative translational products were shown below the mRNA. The putative *CylF* protein had 214 amino acids, which was only 67.5% comparing to the complete sequences. C) The DDE motif of IS from  $\alpha$  hemolytic isolates and other IS3 family members. The accession numbers were shown below the name of IS. Amino acids forming part of the conserved motif were shown as large bold letters with shaded boxes. The numbers in parentheses showed the distance in amino acids between the amino acids of the conserved motif.

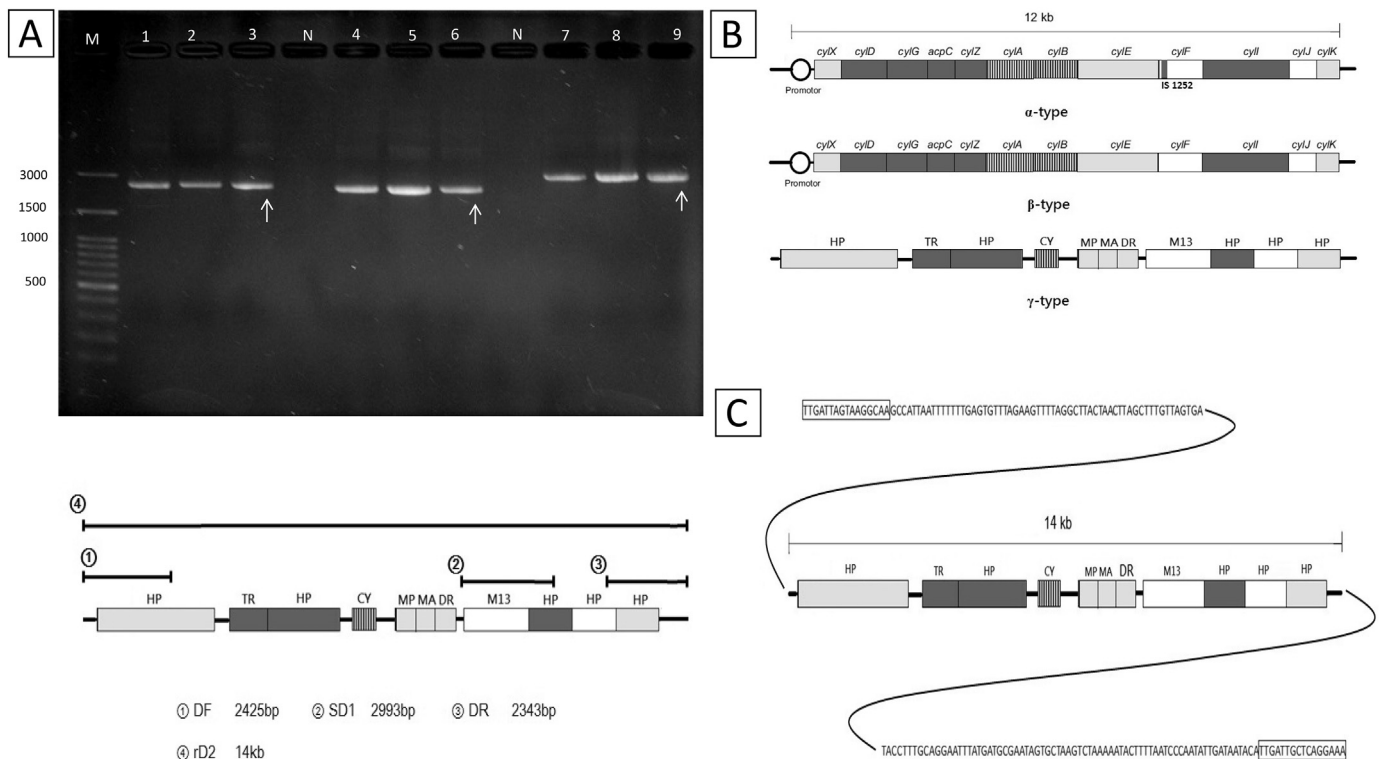


**Fig. 7.** A) Identification of 14 kb DNA of  $\gamma$  hemolytic isolates by nested-PCR with primer DF, DR and SD1. 14 kb gene product (primer rD2) of  $\gamma$  hemolytic genome strain 2-22 (FO393392) was used as template. Lane 1–3 were  $\gamma$  hemolytic isolates 0815-3, T2G and TN using primer DF. Lane 4–6 were the same 1–3  $\gamma$  hemolytic isolates but used primer DR. Lane 7–9 were the same 1–3  $\gamma$  hemolytic isolates but used primer SD1. N was the negative control. Positive amplicons 2425-bp, 2343-bp and 2993-bp of primer DF, DR and SD1 were identified (arrow) in all  $\gamma$  hemolytic isolates. B) Comparison of 14 kb gene products from  $\alpha$ ,  $\beta$  and  $\gamma$  hemolytic isolates. The product of  $\gamma$  hemolytic isolates completely replaced the whole *cyl* operon. C) The 14 kb gene product of  $\gamma$  hemolytic isolates showed genomic island characteristics. It was flanked by 16-bp nearly perfect direct repeats (open boxes), and contained multiple gene regions encoding products with unknown or predicted functions. These predicted products were indicated as following abbreviations: HP (hypothetical protein), TR (transcriptional regulator), CY (cyclic nucleotide-binding protein), MP (membrane protein), MA (septum formation protein Maf), DR (DNA recombinase) and M13 (peptidase M13).

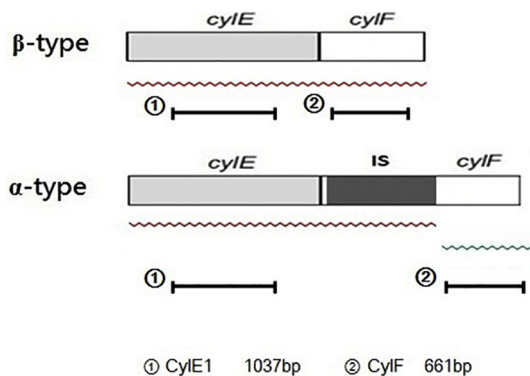


**Fig. 8.** Structure of the *CyIE1* and *CyIF* regions in  $\alpha$  and  $\beta$  hemolytic. The *cyl* operon included *cyIE* and *cyIF*. Insertion sequence region was marked as IS. Transcribed mRNA was shown as meander lines. The  $\alpha$ -type hemolytic *CyIE1* and *CyIF* had transcribed two mRNA. Primer *CyIE1* and *CyI* annealed to mRNA templates in  $\alpha$  and  $\beta$  hemolytic but the  $\alpha$ -type hemolytic annealed to different mRNA templates.

### 3.5. Identification $\gamma$ hemolytic isolates by nested-PCR

The amplification of the primer CovS/R showed no differences among three hemolytic isolates. Regarding sequence analysis,  $\alpha$ - and  $\beta$ -hemolytic isolates showed identity with the genome strain CNCTC 10/84, whereas  $\gamma$ -hemolytic showed identity with genome strain 2-22 (FO393392). PCR products of the entire *cyl* operon was identified by approximately 14-kb-long DNA products for all three hemolytic

isolates. The 14-kb products were further confirmed through nested PCR. For  $\gamma$ -hemolytic isolates, three primers (DF, DR, and SD1) designed from the reference genome strain 2-22 (FO393392) showed positive identification (Fig. 7A), suggesting that the genome of  $\gamma$ -hemolytic isolates could share similarity with genome strain 2-22. The sequence identification of a 14-kb gene fragment of  $\gamma$ -hemolytic isolates showed identity with GIF2 in the genome strain 2-22. This 14-kb GI had completely replaced the entire *cyl* operon, thus leading to  $\gamma$  hemolysis (Fig. 7B). It was flanked by 16-bp-long, almost perfect direct repeats and contained multiple gene regions encoding products with unknown or predicted functions (Fig. 7C).

### 3.6. Detection of different hemolytic isolates by reverse transcription PCR

To evaluate whether the observed phenotypic changes resulted from transcription changes, reverse transcription PCR was performed. The positive amplicons are validated as *CyIE1*, *CyIF*, *CyIES*, *CyIIR*, and *CyIJKr* primers for  $\alpha$ -hemolytic isolates and *CyIE1*, *CyIF*, *CyIIS*, *CyIIR*, and *CyIJKr* primers for  $\beta$ -hemolytic isolates. These results are in accordance with the assumption that the  $\alpha$ -hemolytic isolates could transcribe two strains of mRNA. In the cases of primers *CyIE1* and *CyIF*, the *cyIE* regions upstream of the IS sites could be normally transcribed in both  $\alpha$ - and  $\beta$ -hemolytic isolates. The *cyIF* region downstream of the IS site could not be transcribed normally because of the termination of transcription on IS site; however, our data showed a contradictory result for the  $\alpha$ -hemolytic isolates. The *cyIF* region downstream of the IS site could be amplified in the  $\alpha$ -hemolytic isolates because it transcribed another mRNA (Fig. 8). The positive result of the primer *CyIES* for the  $\alpha$ -hemolytic isolates indicated that the IS region could also be

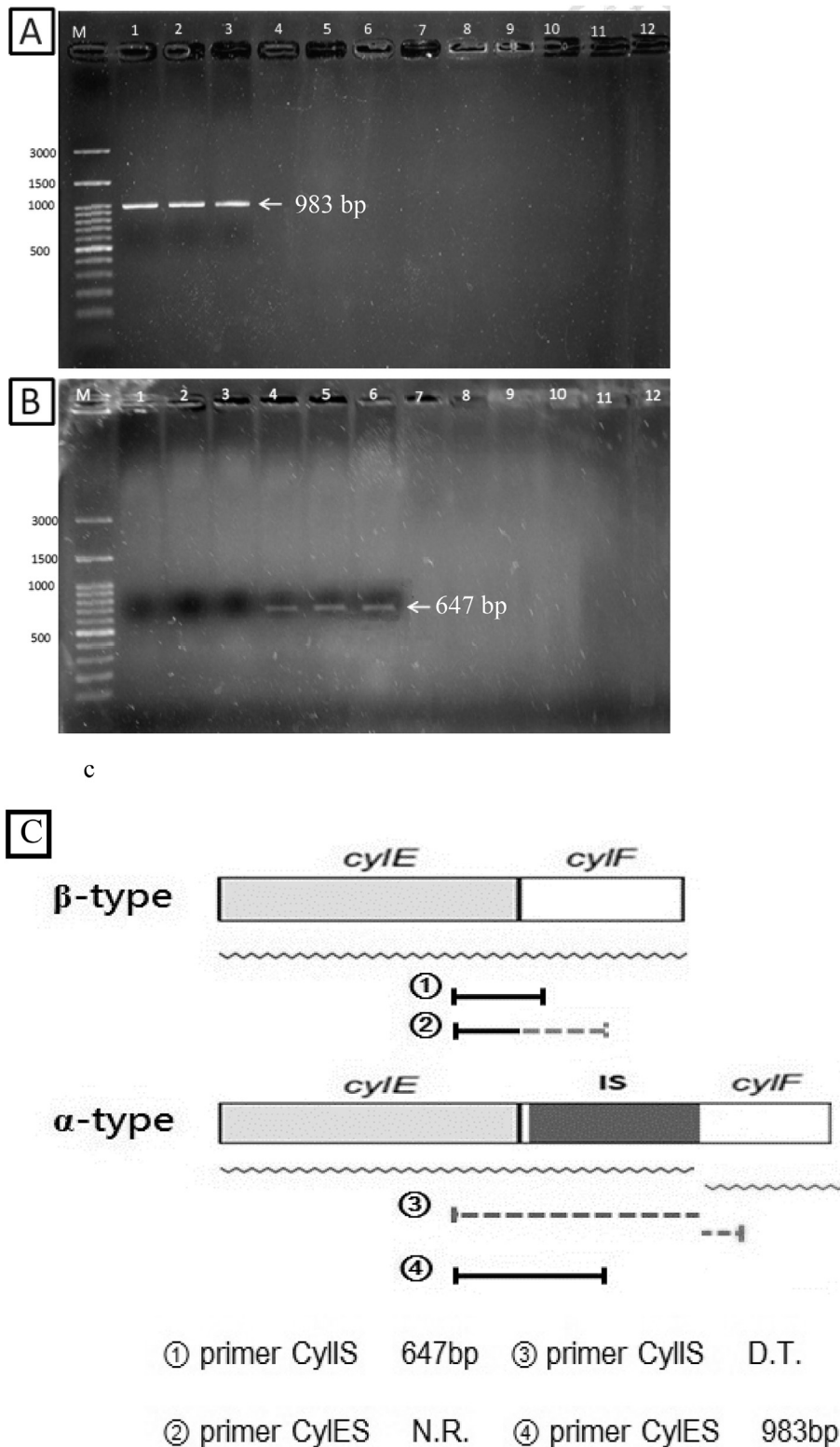


**Fig. 9.** Detection of  $\alpha$  and  $\beta$  hemolytic cDNA using reverse transcription-PCR. Agarose gel electrophoresis of PCR product: lane 1–3  $\alpha$  hemolytic isolates KS, TN681, TN722; lane 4–6  $\beta$  hemolytic isolates 0726–7, 0728–4, 0728–5; lane 7–9  $\alpha$  hemolytic negative control; lane 10–12  $\beta$  hemolytic negative control. Two PCR products of 983-bp and 647-bp. (A) PCR product of 983-bp was generated from the primer set primer *CyES*. (B) PCR product of 647-bp was generated from the primer set primer *CyIIIS*. (C) Structure of the *CyIE1* and *CyIF* regions in  $\alpha$  and  $\beta$  hemolytic. Insertion sequence region was marked as IS. Transcribed mRNA was shown as meander lines. The  $\alpha$ -type hemolytic *CyI* gene had transcribed two mRNA. N.R. suggested “No reverse primer binding site”. D.T. suggested “Different templates”. Primer *CyIES* could anneal to template mRNA in  $\alpha$  hemolytic isolates but the reverse primer binding site of primer *CyIES* didn’t exist in  $\beta$  hemolytic isolates, leading to negative result of amplification. Primer *CyIIIS* could anneal to template mRNA in  $\beta$  hemolytic isolates but the forward and reverse primer of *CyIIIS* annealed to different  $\alpha$  hemolytic isolates of mRNA, respectively, leading to negative result of amplification.

transcribed. The negative result of the primer *CyIIIS* for the  $\alpha$ -hemolytic isolates suggested that the forward and reverse primers annealed to different mRNA templates. Thus, the reaction could not be performed (Fig. 9). Finally, the primers *CyIIr* and *CyIJKr* showed positive amplicons for in both  $\alpha$ - and  $\beta$ -hemolytic isolates. These positive results in  $\alpha$ -hemolytic isolates indicated that *cyl* regions downstream of the IS site could be transcribed consecutively (Fig. 10).

#### 4. Discussion

In this study, 45 isolates were collected from different fish farms with a GBS infection outbreak from 2009 to 2014. These GBS colonies differed in the phenotypic properties associated with their virulence factors,  $\beta$ -h/c cytotoxin, and exopolysaccharide capsule. Three hemolytic types— $\alpha$ ,  $\beta$ , and  $\gamma$ —were identified. Based on our survey and literature findings, few  $\alpha$ -hemolytic isolate in aquaculture animals has

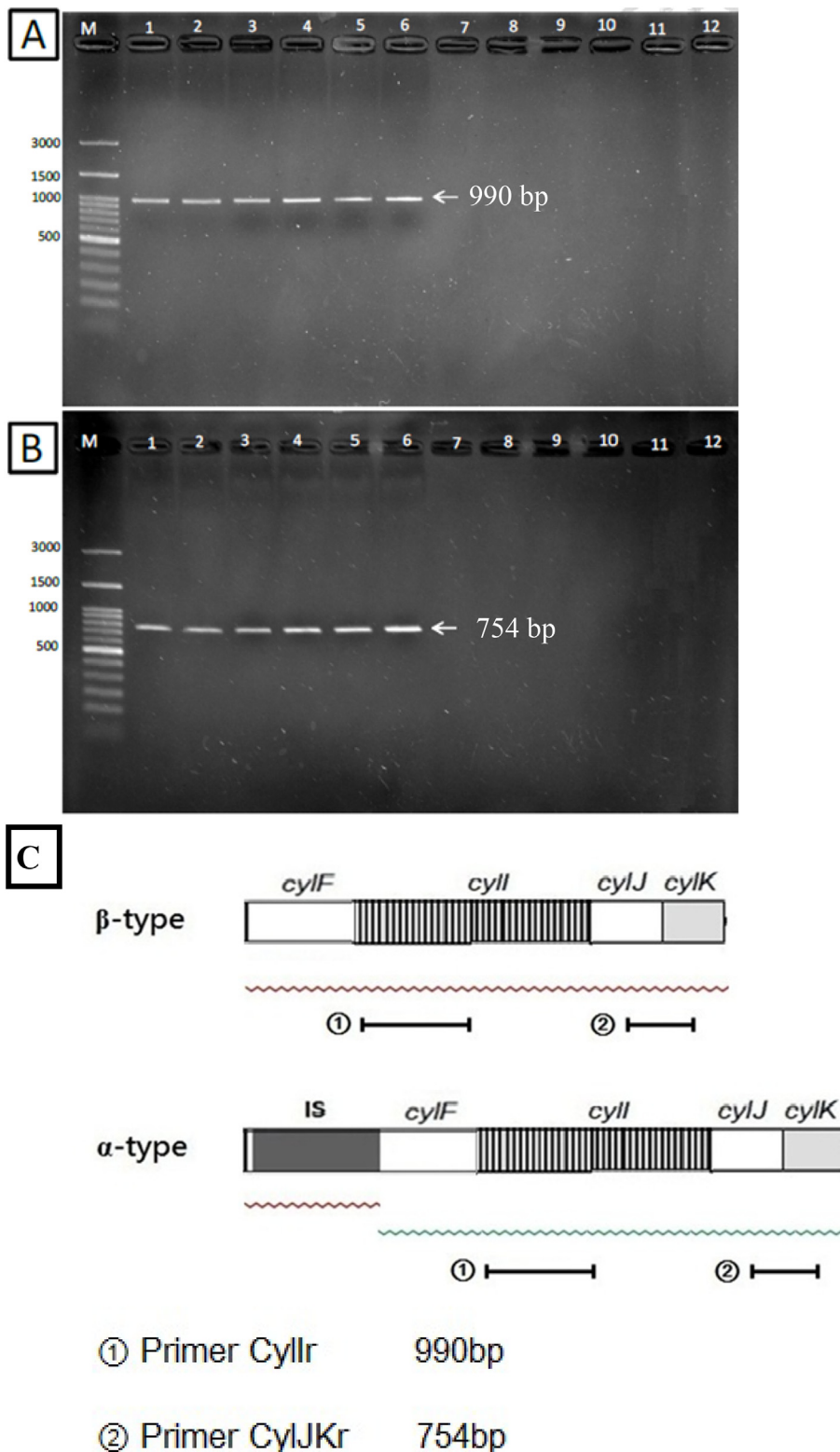


**Fig. 10.** Detection of  $\alpha$  and  $\beta$  hemolytic cDNA using reverse transcription-PCR. Agarose gel electrophoresis of PCR product: lane 1–3  $\alpha$  hemolytic isolates KS, N681, TN722; lane 4–6  $\beta$  hemolytic isolates 0726–7, 0728–4, 0728–5; lane 7–9  $\alpha$  hemolytic negative control; lane 10–12  $\beta$  hemolytic negative control. Two PCR products of 983-bp and 647-bp. (A) PCR product of 990-bp was generated from the primer set primer CylIr. (B) PCR product of 754-bp was generated from the primer set primer CylJK. (C) Structure of the *cyl* gene regions in  $\alpha$  and  $\beta$  hemolytic. *Cyl* gene regions included *cylF*, *cylI*, *cylJ* and *cylK*. Insertion sequence region was marked as IS. Transcribed mRNA was shown as meander lines. The  $\alpha$ -type hemolytic *cyl* gene had transcribed two mRNA. Primer CylIr and CylJKr could anneal to template mRNA in both  $\alpha$  and  $\beta$  hemolytic isolates but primers in the case of  $\alpha$  hemolytic isolates annealed to another transcribed mRNA downstream of the insertion site.

been reported. The  $\gamma$ -hemolytic isolates had thicker encapsulation but slower growth than did the  $\alpha$ - and  $\beta$ -hemolytic isolates. Therefore, sequence differences in the gene clusters leading to these phenotypic variations were explored. None of the three isolate types demonstrated mutation in the regulatory gene *covS/R*. However, gene mutation in the  $\alpha$ - and  $\gamma$ -hemolytic isolates indicated that the phenotype switch in both isolates might be due to the mutation in their hemolysis-associated gene cluster, the *cyl* operon.

Sequence analysis of *cyl* operon genes showed that a 1252-bp insertion in the *cylF* gene of the  $\alpha$ -hemolytic phenotype reduced bacteria hemolytic activity. By contrast, Spellerberg et al. (1999, 2000) demonstrated that an IS in the *cyl* operon could result in the loss of hemolysis. To explore whether genes downstream of the IS site could be transcribed, mRNA transcripts were produced using reverse transcription PCR. After analysis, we hypothesized that genes downstream of the IS site could be still transcribed because of a new promoter discovered

just at the IS site. All genes, including *cylI*, *cylJ*, and *cylK*, could be transcribed intact, except for *cylF*. The putative translation sequence of CylF was incomplete, and only 67.5% of it was preserved. CylF works as a putative aminomethyltransferase during  $\beta$ -hemolysin synthesis; CylF is believed to be responsible for the production of methylated derivatives of  $\beta$ -hemolysin (Whidbey et al. 2013). However, whether these methylated derivatives are necessary for  $\beta$ -hemolysis and how it reacts to cause hemolytic activity remains unknown. Thus, we propose that incomplete CylF leads to the malfunction of methylated derivatives and affects the hemolytic activity, finally contributing to the switch of the hemolytic phenotype.

In the  $\gamma$ -hemolytic isolates, a complete deletion and replacement of *cyl* operon by a 14-kb GI was noted. Sequence analysis of this GI showed identity with the genome of *S. agalactiae* strain 2–22. This strain was first isolated from trout in Israel (Eldar et al. 1994, 1995). In addition to the genome sequence, many characteristics of the GBS strain 2–22 are similar to those of our  $\gamma$ -hemolytic isolates, such as serotype, thick encapsulation, and absence of hemolysis. According to multilocus sequence typing, GBS strain 2–22 belongs to sequence type (ST) 261 (Rosinski-Chupin et al. 2013). ST261 was only discovered in fish and had many genetic defects comparing to the strains found in human (Delannoy et al. 2013). These genetic defects associated with hemolysis, energy metabolism, transport, binding, regulation, and signal transduction might result from the adaptation of these organisms to fish species (Rosinski-Chupin et al. 2013). Thus, the genetic defects in our  $\gamma$ -hemolytic isolates potentially explain their phenotypic conversion.

Sequence alignment of the GI in  $\gamma$ -hemolytic isolates showed that multiple gene regions with predicted or unknown function comprised a 14-kb GI. Some of them may be related to the phenotypic variation of  $\gamma$ -hemolytic isolates. For instance, in the  $\gamma$ -hemolytic isolates, transcriptional regulator and cyclic nucleotide-binding proteins may have a role in upregulating encapsulation, causing the thicker encapsulation. Moreover, the septum formation protein Maf seems to induce the growth rate reduction observed in the  $\gamma$ -hemolytic isolates. A study demonstrated that the introduction of *maf* in a multicopy plasmid into *Bacillus subtilis* resulted in extensive filamentation caused by the disruption and subsequent inhibition of the septation process (Butler et al. 1993). Another research demonstrated that Maf inhibits the synthesis of the division septum, delaying the outgrowth in *B. subtilis* (Hamoen 2011). The inhibitory effect of Maf on *S. agalactiae* potentially delayed the growth of the  $\gamma$ -hemolytic isolates.

Among the three isolate types, the  $\gamma$ -hemolytic isolates demonstrated the most phenotypic variation. The relative slow growth rate of the  $\gamma$ -hemolytic isolates might be due to the 14-kb GI or other potential genetic defects related to energy metabolism or transportation. The loss of hemolysis in  $\gamma$ -hemolytic isolates was due to complete deletion of the *cyl* operon; this defect might have affected encapsulation as well. The complete elimination of  $\beta$ -h/c by targeted mutagenesis can diminish GBS resistance to phagocytic killing (Liu et al. 2004) and reduce its survival in various animal models (Doran et al. 2003; Hensler et al. 2005; Puliti et al. 2000). Our  $\gamma$ -hemolytic isolates demonstrated hyperencapsulation to potentially impair opsonophagocytosis and enhance resistance (Herbert et al. 2004). The upregulation of encapsulation in  $\gamma$ -hemolytic isolates might be controlled by the transcriptional regulator in the 14-kb GI or by other two-component regulatory systems because *covS/R* did not seem to be upregulating encapsulation.

## 5. Conclusions

In summary, we studied three hemolytic phenotypes of GBS isolates:  $\alpha$ ,  $\beta$ , and  $\gamma$ . The  $\beta$ -hemolytic isolates were standard GBS strains and thus used as control for the other two types. The  $\alpha$ -hemolytic isolates demonstrated incomplete hemolysis, resulting from a 1252-bp IS in the *cylF* region. The  $\gamma$ -hemolytic isolates showed a complete loss of hemolytic activity because of the total deletion of the *cyl* operon and replacement by a 14-kb GI. Other phenotypic variations of  $\gamma$ -hemolytic

isolate, such as delayed growth rate and thick encapsulation, might also be associated with the GI. While mutation occurred might decrease the virulence and increase the probability of the bacterial survival in fish and causing less causality. However, gene mutation in the *cyl* operon leads to the emergence of different GBS phenotype isolates. These GBS phenotypic variants may be essential in the future analysis of the molecular pathogenesis of GBS in diagnostic microbiology.

## Acknowledgements

We acknowledge those fish farms for providing samples and laboratory technicians for helping with this study.

## References

- Brown, T., 2006. Gene Cloning and DNA Analysis: An Introduction. Blackwell Pub, Cambridge, MA.
- Butler, Y.X., Abhayawardhane, Y., Stewart, G.C., 1993. Amplification of the *Bacillus subtilis* maf gene results in arrested septum formation. J. Bacteriol. 175, 3139–3145.
- Delannoy, C.M.J., Crumlish, M., Fontaine, M.C., Pollock, J., Foster, G., Dagleish, M.P., Turnbull, J.F., Zadoks, R.N., 2013. Human *Streptococcus agalactiae* strains in aquatic mammals and fish. BMC Microbiol. 13, 41.
- Domeenech, A., Derenaandez, G.J., Pacual, C., Garcia, J., Cutuli, M., Moreno, M., Collin, M., Dominguez, L., 1996. Streptococcosis in cultured turbot, *Scophthalmus maximus* (L.), associated with *Streptococcus parauberis*. J. Fish Dis. 19, 33–38.
- Doran, K.S., Liu, G.Y., Nizet, V., 2003. Group B streptococcal beta-hemolysin/cytolysin activates neutrophil signaling pathways in brain endothelium and contributes to development of meningitis. J. Clin. Invest. 112, 736–744.
- Edwards, M.S., Nizet, V., 2011. Group B streptococcal infections. In: Remington, J.S., Klein, J.O., Wilson, C.B., Nizet, V., Maldonado, Y.A. (Eds.), Infectious Diseases of the Fetus and Newborn Infant, 7th ed. Elsevier, Amsterdam, pp. 419–469.
- Eldar, A., Bejerano, Y., Bercovier, H., 1994. *Streptococcus shiloi* and *Streptococcus difficle*: two new streptococcal species causing a meningoencephalitis in fish. Curr. Microbiol. 28, 139–143.
- Eldar, A., Bejerano, Y., Livoff, A., Horovitz, A., Bercovier, H., 1995. Experimental streptococcal meningo-encephalitis in cultured fish. Vet. Microbiol. 43, 33–40.
- Evans, J.J., Wiedenmayer, A.A., Klesius, P.H., Shoemaker, C.A., 2004. Survival of *Streptococcus agalactiae* from frozen fish following natural and experimental infections. Aquaculture 233, 15–21.
- Garcia, J.C., Klesius, P.H., Evans, J.J., Shoemaker, C.A., 2008. Non-infectivity of cattle *Streptococcus agalactiae* in Nile tilapia, *Oreochromis niloticus* and channel catfish, *Ictalurus punctatus*. Aquaculture 281, 151–154.
- Hamoen, L.W., 2011. Cell division blockage: but this time by a surprisingly conserved protein. Mol. Microbiol. 81, 1–3.
- Hensler, M.E., Liu, G.Y., Sobczak, S., Benirschke, K., Nizet, V., Heldt, G.P., 2005. Virulence role of group B *Streptococcus* beta-hemolysin/cytolysin in a neonatal rabbit model of early-onset pulmonary infection. J. Infect. Dis. 191, 1287–1291.
- Herbert, M.A., Beveridge, C.J., Saunders, N.J., 2004. Bacterial virulence factors in neonatal sepsis: group B streptococcus. Curr. Opin. Infect. Dis. 17, 225–229.
- Imperi, M., Pataracchia, M., Alfarone, G., Baldassarri, L., Orefici, G., Creti, R., 2010. A multiplex PCR assay for the direct identification of the capsular type (Ia to IX) of *Streptococcus agalactiae*. J. Microbiol. Method. 80, 212–214.
- Jiang, S.M., Gieslewicz, M.J., Kasper, D.L., Wessels, M.R., 2005. Regulation of virulence by a two-component system in group B streptococcus. J. Bacteriol. 187, 1105–1113.
- Koskiniemi, S., Sellin, M., Norgren, M., 1998. Identification of two genes, *cpsX* and *cpsY*, with putative regulatory function on capsule expression in group B streptococci. FEMS Immunol. Med. Microbiol. 21, 159–168.
- Lamy, M.C., Zouine, M., Fert, J., Vergassola, M., Couve, E., Pellegrini, E., Glaser, P., Kunst, F., Msadek, M., Trieu-Cuot, P., Poyart, C., 2004. *CovS/CovR* of group B *Streptococcus*: a two-component global regulatory system involved in virulence. Mol. Microbiol. 54, 1250–1268.
- Liu, G.Y., Doran, K.S., Lawrence, T., Turkson, N., Puliti, M., Tissi, L., Nizet, V., 2004. Sword and shield: linked group B streptococcal beta-hemolysin/cytolysin and carotenoid pigment function to subvert host phagocyte defense. Proc. Natl. Acad. Sci. U. S. A. 101, 14491–14496.
- Nizet, W., Gibson, R.L., Chi, E.M., Framson, P.E., Hulse, M., Ribens, C.E., 1996. Group B streptococcal beta-hemolysin expression is associated with injury of lung epithelial cells. Infect. Immun. 64, 3818–3826.
- Poyart, C., Tazi, A., Réglie-Poupet, H., Billoët, A., Tavares, N., Raymond, J., Trieu-Cuot, P., 2007. Multiplex PCR assay for rapid and accurate capsular typing of group B streptococci. J. Clin. Microbiol. 45, 1985–1988.
- Puliti, M., Nizet, V., von Hunolstein, C., Bistoni, F., Mosci, P., Orefici, G., Tissi, L., 2000. Severity of group B streptococcal arthritis is correlated with beta-hemolysin expression. J. Infect. Dis. 182, 824–832.
- Rodriguez-Granger, J., Alvargonzalez, J.C., Berardi, A., Berner, R., Kunze, M., Hufnagel, M., Melin, P., Decheva, A., Orefici, G., Poyart, C., Telford, J., Efstratiou, A., Killian, M., Krizova, P., Baldassarri, L., Spellerberg, B., Puertas, A., Rosa-Fraile, M., 2012. Prevention of group B streptococcal neonatal disease revisited. The DEVANI European project. Eur. J. Clin. Microbiol. Infect. Dis. 31, 2097–2104.
- Rosinski-Chupin, I., Sauvage, E., Mairey, B., Mangenot, S., Ma, L., Cunha, V.D., Rusniok, C., Bouchier, C., Barbe, V., Glaser, P., 2013. Reductive evolution in *Streptococcus*

- agalactiae* and the emergence of a host adapted lineage. BMC Genomics 14, 252.
- Sigge, A., Schmid, M., Maurer, S., Spellerberg, B., 2008. Heterogeneity of hemolysin expression during neonatal *Streptococcus agalactiae* sepsis. J. Clin. Microbiol. 46, 807–809.
- Spellerberg, B., Pohl, B., Haase, G., Martin, S., Weber-Heynemann, J., Lütticken, R., 1999. Identification of genetic determinants for the hemolytic activity of *Streptococcus agalactiae* by ISS1 transposition. J. Bacteriol. 181, 3212–3219.
- Spellerberg, B., Martin, S., Franken, C., Berner, R., Lütticken, R., 2000. Identification of a novel insertion sequence element in *Streptococcus agalactiae*. Gene 241, 51–56.
- Tapsall, J.W., Phillips, E.A., 1991. The hemolytic and cytolytic activity of group B streptococcal hemolysin and its possible role in early onset group B streptococcal disease. Pathology 23, 139–144.
- Verani, J.R., McGee, L., Schrag, S.J., 2010. Prevention of perinatal group B streptococcal disease revised guidelines from CDC. MMWR Recomm. Rep. 59, 1–32.
- Whidbey, C., Harrell, M.I., Burnside, K., Ngo, L., Becraft, A.K., Iyer, L.M., Aravind, L., Hitti, J., Waldorf, K.M.D., Rajagopal, L., 2013. A hemolytic pigment of Group B *Streptococcus* allows bacterial penetration of human placenta. J. Exp. Med. 210, 1265–1281.
- Yanong, R.P.E., Francis-Floyd, R., 2010. Streptococcal Infections of Fish. 57 IFSA, University of Florida, Circular.